Universal Journal of Mechanical Engineering 2(7): 211-219, 2014 http://www.hrpub.org
DOI: 10.13189/ ujme.2014.020701

Parametric Study of Double Link Flexible Manipulator

S. Mahto*, U.S. Dixit

Department of Mechanical Engineering, Indian Institute of Technology, Guwahati, Assam
*Corresponding Author: smh@iitg.ernet.in

Abstract In this work, finite element method based on Lagrangian formulation is used for obtaining the equations of motion of the double link flexible revolute-jointed robotic manipulator. Both the links are considered as Euler-Bernoulli beams. A parametric study is carried out for the double link flexible robotic manipulator through linear modeling technique. A comparative study for dynamic response is carried out for the uniform beam manipulators under various types of excitations.

Keywords Double Link Flexible Manipulator, Euler-Bernoulli Beam, Finite Element Method, Lagrange Technique

1. Introduction

In conventional robotic system, links are rigid giving small static deflection and hence it is possible to obtain high positional accuracy. However, most of the power is used to overcome the inertia of the system. On other hand, lightweight and large dimension robotic manipulators have become popular due to their higher manipulation speed, less weight/overall cost, transportability, better energy consumption, enhanced payload capacity etc in comparison to conventional robotic system. There is a wide range of applications of such new generation robotic systems in many areas nowadays. It is desired to design lighter robots to carry out heavier payloads as well as to operate it at higher speeds. Thus, flexible link manipulators are a subject of intensive research.

Dwivedy and Eberhard (2006) presented a wide review on dynamic analysis of flexible manipulator done by various researchers. Book *et al.* (1975) linearized the equations of motion about a nominal configuration for a two-link flexible manipulator. Chang and Hamilton (1991), and Usoro *et al.* (1986) presented a Lagrangian finite element approach for the mathematical modeling of the manipulators with flexible links. Yigit (1994) modeled a two-link rigid-flexible manipulator and derived the equations of motion by applying the Hamilton's principle. Ankarah and Diken (1997) used the Euler–Bernoulli beam theory and solved the transient vibration theorem with the mode summation method to control the residual vibration of a single flexible link.

The dynamics of a flexible arm and flexible joint manipulator carrying a payload with rotary inertia was studied by Bedoor and Almusallam (2000). Meghdari and Fahimi (2001) derived the improved elastic generalized coordinates. Kane's equation of motion for arbitrary number of rigid and elastic bodies is presented. Also, equations of motion are de-coupled in first order terms. Zhang and Bai (2012) established Lagrangian dynamic equations of two-link flexible manipulator through integrated model and multi body dynamics method. Dynamic response reliability is analyzed by using Monte Carlo and extremum surface method.

Most of the published work focuses on modelling and pays less attention for its optimal design. Asada *et al*. (1991) presented optimum structure along with control aspect of flexible robot arms. Coordinates used by finite element model are treated as design variables, which are optimized for obtaining the optimal shape and structure of the arm mechanism. Wang (1994) addressed optimum design of a single link manipulator to maximize its fundamental frequency. He formulated the design problem as a nonlinear eigenvalue problem and used variational method. He demonstrated the increase of fundamental frequency as a result of optimization by considering a few numerical examples.

In the present work a linearized model for small rigid body motion and small flexural deflection is used. Based on this model, complete parametric study is done to predict the dynamic behaviour of the system due to the variation of various design parameters. In addition, shape optimization is done to increase the fundamental frequency and dynamic response of the optimized links is studied.

Nomenclature

$1, 2$	subscripts defined for first link and second link respectively
E_1, E_2	Young's modulus
$h_1,\ h_2$	elements lengths
I_1, I_2	second moments of inertia
$[K]$	global stiffness matrix
$[K_1^i], [K_2^j]$	elemental stiffness matrices of i^{th} and j^{th} elements respective
L_1, L_2	Link length
$m_1,\ m_2$	masses per unit length
m_{t_1}, m_{t_2}	tip loads (payloads)
$[M]$	global inertia matrix
$[M_1^i], [M_2^j]$	elemental inertia matrices of i^{th} and j^{th} elements respectively
n_1, n_2	no of finite elements
q	global nodal variables or generalized co-ordinates
$r_1, r_1^{'}$	position vectors of point $P_1^{'}$ in link 1 with respect to XOY and X_1OY_1
$r_2, r_2^{'}$	position vectors of point $P_2^{'}$ in link 2 with respect to XOY and X_1OY_1
$u_{2i},\ u_{2i+2}$	deflections at node of ith element of 1st link
$u_{2i-1},\ u_{2i+1}$	slopes at node of ith element of 1st link
w_{2j-1}, w_{2j+1}	slopes at node of jth element of 2nd link
XOY	inertial system of co-ordinate
X_1OY_1	body-fixed system of co-ordinate attached to link 1
$X_1^{'}O_2Y_1^{'}$	lateral transformation of X_1OY_1 by $((L_1, u_{2n1+1})$
$X_2O_2Y_2$	body fixed to the system of co-ordinate attached in link2
α	ratio of length of second link to that of first link
β	ratio of hub mass to the total mass of the links
μ_1, μ_2	ratio of payload to the total mass of the links
ρ_1, ρ_2	specific densities
τ_1, τ_2	applied torques at hub and link joint respectively

2. Obtaining Elemental Equation of Manipulator

Rotating flexible beams have significant transverse deflections. They behave as a nonlinear elastic beams and exhibit vibratory motions in both chord wise and flap wise directions. However, Robotic manipulators usually work at moderate peak speed. Induced transverse force in the chord wise direction due to the applied excitation torque is much higher compared to the gravity force in flap wise direction and vibrations are predominantly in chord wise directions. In this work, model of Usoro *at el.* (1986) is adopted. However, formulations are consistently linearized for small angular/transverse deflections under linear beam theory to reduce the complexity of the system modeling.

2.1 Modeling of First Link

Fig.1(a) shows single link flexible manipulator in which XOY and X_1OY_1 represents the stationary and moving co-ordinate frames respectively. Motion of the link is represented by fixed XOY co-ordinate frame. The link is

considered slender. Hence, transverse shear and rotary inertia effects are neglected allowing it to be treated as an Euler-Bernoulli beam. Beam is assumed to vibrate predominantly in horizontal plane (XOY), neglecting gravity effects.

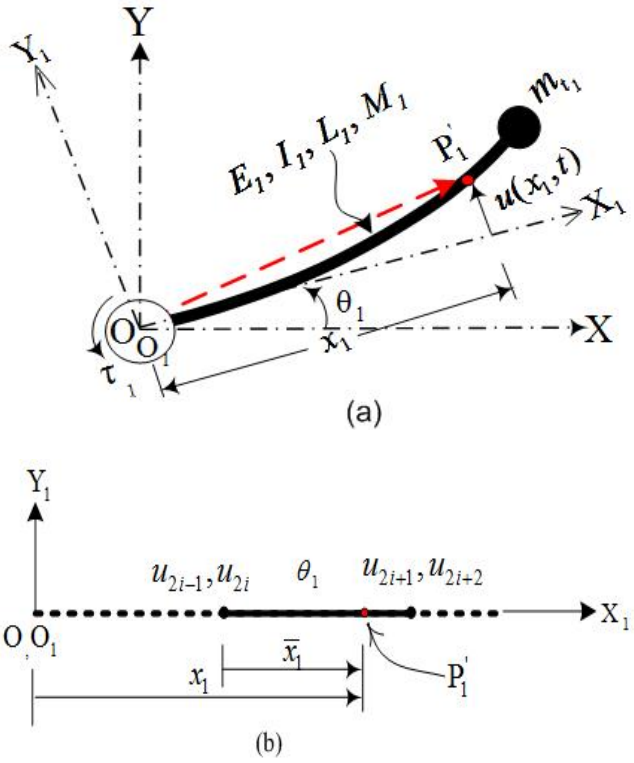

Figure 1. (a) Configuration diagram of 1st link of manipulator

(b) Typical i^{th} finite element of the 1st link having 5 dof

Consider a point P_1 in the i^{th} element on the manipulator at a distance x_1 from the hub. The point P_1 attains the position P_1' with respect to inertial frame of reference (XOY) after having rigid body motion $\theta_1(t)$ and flexural deflection $u(x_1,t)$. Flexural deflection $u(x_1,t)$ of point P_1 is approximated as

$$u(x_1,t) = N_1u_{2i-1} + N_2u_{2i} + N_3u_{2i+1} + N_4u_{2i+2} = \lfloor N \rfloor \{U\} \quad (1)$$

Where

$$\lfloor N \rfloor = \lfloor N_1 \; N_2 \; N_3 \; N_4 \rfloor,$$

$$\{U\}^T = \lfloor u_{2i-1} \quad u_{2i} \quad u_{2i+1} \quad u_{2i-2} \rfloor.$$

In the FEM formulation the manipulator is divided into finite elements, each element having five degrees of freedom. Detail of i^{th} element of the first link is shown in Fig. 1(b). In the figure, θ_1 is the hub rotation and u_{2i-1}, u_{2i}, u_{2i+1} and u_{2i+2} are the transverse deflections and slopes at the first and second nodes of the element. The position vector of P_1' with respect to inertial system XOY for smaller angular displacement and small flexural deflection is given by

$$r_1 = \begin{bmatrix} X \\ Y \end{bmatrix} = \begin{bmatrix} x_1 \\ \theta_1 x_1 + u \end{bmatrix}. \quad (2)$$

In finite element method, variables are converted to nodal variables.

Let

$$Z_1 = \lfloor \theta_1 \quad u_{2i-1} \quad u_{2i} \quad u_{2i+1} \quad u_{2i+2} \rfloor,$$

then

$$\frac{\partial r_1}{\partial t} = \left\lfloor \frac{\partial r_1}{\partial Z_1} \right\rfloor \dot{Z}_1^T \quad (3)$$

2.1.1. Kinetic energy computation of the i[th] element of the 1[st] link:

Kinetic energy of i^{th} element of the first link is given by

$$T_1^i = \frac{1}{2}\int_0^{h_1} m_1 \left[\frac{\partial r_1^T}{\partial t} \cdot \frac{\partial r_1}{\partial t} \right] d\bar{x}_1. \quad (4)$$

We have

$$\frac{\partial r_1^T}{\partial t} \cdot \frac{\partial r_1}{\partial t} = \dot{Z}_1^T \left[\frac{\partial r_1}{\partial Z_1} \right]^T \left[\frac{\partial r_1}{\partial Z_1} \right] \dot{Z}_1 \quad (5)$$

Substituting Equation 5 in Equation 4, we get

$$T_1^i = \frac{1}{2}\dot{Z}_1^T \left[\int_0^{h_1} m_1 \left[\frac{\partial r_1}{\partial Z_1} \right]^T \cdot \left[\frac{\partial r_1}{\partial Z_1} \right] d\bar{x}_1 \right] \dot{Z}_1. \quad (6)$$

Thus elemental mass matrix is given by

$$M_1^i = \int_0^{h_1} m_1 \left[\frac{\partial r_1}{\partial Z_1} \right]^T \cdot \left[\frac{\partial r_1}{\partial Z_1} \right] d\bar{x}_1 = \begin{bmatrix} M_{11} & M_{12} & M_{13} & M_{14} & M_{15} \\ M_{21} & & & & \\ M_{31} & & & & \\ M_{41} & & P_{1i} & & \\ M_{51} & & & & \end{bmatrix}, \quad (7)$$

where,

$$P_{1i} = \frac{m_1 h_1}{420} \begin{bmatrix} 156 & 22h_1 & 54 & -13h_1 \\ 22h_1 & 4h_1^2 & 13h_1 & -3h_1^2 \\ 54 & 13h_1 & 156 & -22h_1 \\ -13h_1 & -3h_1^2 & -22h_1 & 4h_1^2 \end{bmatrix}$$

All the constants of the above matrix may be obtained by integrating M_1^i for different vector elements of Z_1.

2.1.2. Elastic potential energy of the i[th] element of 1[st] link

Potential energy of the i^{th} element of 1[st] link due to elastic deformation is given by

$$V_1^i = \frac{1}{2}\int_0^{h_1} E_1 I_1 \left[\frac{\partial^2 u}{\partial x_1^2}\right]^2 \mathrm{d}\bar{x}_1 = \{U\}^T \frac{1}{2}\int_0^{h_1} E_1 I_1 \lfloor N'' \rfloor^T \lfloor N'' \rfloor \mathrm{d}\bar{x}_1 \{U\} \quad (8)$$

Thus, elemental stiffness matrix is given by

$$K_1^i = E_1 I_1 \int_0^{h_1} \lfloor N'' \rfloor^T \lfloor N'' \rfloor \mathrm{d}\bar{x}_1 = \frac{E_1 I_1}{h_1^3}\begin{bmatrix} 0 & 0 & 0 & 0 & 0 \\ 0 & 12 & 6h_1 & -12 & 6h_1 \\ 0 & 6h_1 & 4h_1^2 & -6h_1 & 2h_1^2 \\ 0 & -12 & -6h_1 & 12 & -6h_1 \\ 0 & 6h_1 & 2h_1^2 & -6h_1 & 4h_1^2 \end{bmatrix} \quad (9)$$

2.2 Modeling of Second Link

Figure 2(a) shows 2[nd] link flexible manipulator in which XOY represents the stationary and $X_1O_1Y_1, X_2O_2Y_2$ and $X_1'O_2Y_1'$ represent moving co-ordinate frames. Consider an infinitesimal link element P_2 on the manipulator at a distance x_2 from the link joint. Point P_2 attains the position P_2' after time '*t*' with respect to non-inertial frame of reference ($X_2O_2Y_2$) after having rigid body motion $\theta_2(t)$ and transverse deflection $w(x_2,t)$ .Flexural deflection $w(x_2,t)$ of point P_2 is approximated in finite element as

$$w(x_2,t) = S_1 w_{2j-1} + S_2 w_{2j} + S_3 w_{2j+1} + S_4 w_{2j+2} = \lfloor S \rfloor \{W\}, \quad (10)$$

Where $\lfloor S \rfloor = \lfloor S_1 \; S_2 \; S_3 \; S_4 \rfloor$,

$\{W\}^T = \lfloor w_{2j-1} \quad w_{2j} \quad w_{2j+1} \quad w_{2j-2} \rfloor$.

Hermitian shape functions are expressed byS_i.

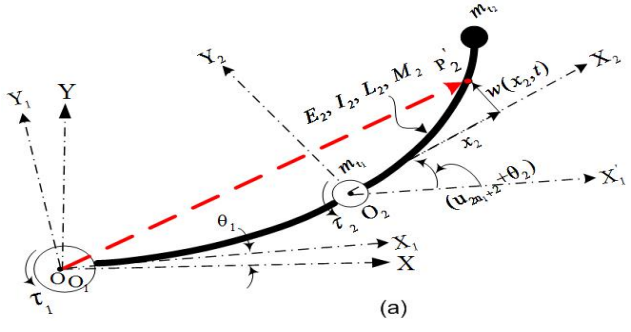

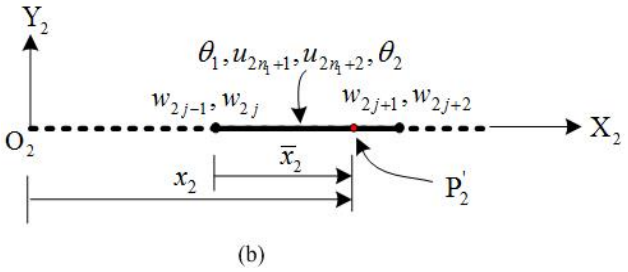

Figure 2. **(a)** Configuration diagram of 2[nd] link of manipulator, **(b)** Typical j^{th} element of the 2[nd] link having 8 dof

In the FEM formulation the manipulator is divided into 10 elements, each element having eight degrees of freedom. Detail of j^{th} element of the second link is shown in Figure 2(b). In the Figure 2b, θ_2 is the second link rotation and $w_{2j-1}, w_{2j}, w_{2j+1}$ and w_{2j+2} are the transverse deflections and slopes at the first and second nodes of the element along with the variables associated with the first link θ_1, u_{2n_1+1} and u_{2n_1+2}. The position vector of P_2' with respect to inertia system XOY for smaller angular displacement and small flexural deflection is given by

$$\boldsymbol{r}_2 = \begin{bmatrix} L_1 + x_2 \\ \theta_1(L_1 + x_2) + u_{2n_1+1} + x_2\theta_2 + x_2 u_{2n_1+2} + w \end{bmatrix}. \quad (11)$$

In finite element, variables are converted to nodal variables. Let

$Z_2 = \lfloor \theta_1 \quad u_{2n_1+1} \quad u_{2n_1+2} \quad \theta_2 \quad w_{2j-1} \quad w_{2j-1} \quad w_{2j-1} \quad w_{2j+1} \rfloor$

then

$$\frac{\partial \boldsymbol{r}_2}{\partial t} = \left\lfloor \frac{\partial \boldsymbol{r}_2}{\partial Z_2} \right\rfloor \dot{Z}_2^T \quad (12)$$

and

$$\frac{\partial \boldsymbol{r}_2^T}{\partial t} \cdot \frac{\partial \boldsymbol{r}_2}{\partial t} = \dot{Z}_2^T \left\{ \left(\frac{\partial \boldsymbol{r}_2}{\partial Z_2} \right)^T \right\} \left\lfloor \frac{\partial \boldsymbol{r}_2}{\partial Z_2} \right\rfloor \dot{Z}_2 \quad (13)$$

2.2.1. Kinetic Energy Computation of the j[th] element of the 2[nd] link:

Kinetic energy of the second link of the j^{th} element is

$$T_2^j = \frac{1}{2}\dot{Z}_2^T \left[\int_0^{h_2} m_2 \left[\frac{\partial \boldsymbol{r}_2}{\partial t}\right]^T \cdot \left[\frac{\partial \boldsymbol{r}_2}{\partial t}\right] \mathrm{d}\bar{x}_2 \right] \dot{Z}_2, \quad (14)$$

Thus, mass matrix of the element become

$$M_2^j = \int_0^{h_2} m_2 \left[\frac{\partial \boldsymbol{r}_2}{\partial t}\right]^T \cdot \left[\frac{\partial \boldsymbol{r}_2}{\partial t}\right] \mathrm{d}\bar{x}_2 \qquad (15)$$

$$M_2{}^j = \begin{bmatrix} M_{11} & M_{12} & M_{13} & M_{14} & M_{15} & M_{16} & M_{17} & M_{18} \\ M_{21} & M_{22} & M_{23} & M_{24} & M_{25} & M_{26} & M_{27} & M_{28} \\ M_{31} & M_{32} & M_{33} & M_{34} & M_{35} & M_{36} & M_{37} & M_{38} \\ M_{41} & M_{42} & M_{43} & M_{44} & M_{45} & M_{46} & M_{47} & M_{48} \\ M_{51} & M_{52} & M_{53} & M_{54} & & & & \\ M_{61} & M_{62} & M_{63} & M_{64} & & P_{2j} & & \\ M_{71} & M_{72} & M_{73} & M_{74} & & & & \\ M_{18} & M_{82} & M_{83} & M_{84} & & & & \end{bmatrix}, \qquad (16)$$

Where

$$P_{2j} = \frac{m_2 h_2}{420} \begin{bmatrix} 156 & 22h_2 & 54 & -13h_2 \\ 22h_2 & 4h_2^2 & 13h_2 & -3h_2^2 \\ 54 & 13h_2 & 156 & -22h_2 \\ -13h_2 & -3h_2^2 & -22h_2 & 4h_2^2 \end{bmatrix}.$$

All the constants of the above matrix may be obtained by integrating M_2^j for different vector elements of Z_2.

2.2.2. Elastic potential energy of the jth element of 2nd Link

The potential energy of the j^{th} element of the 2nd link due to elastic deformation is given as

$$V_2{}^j = \frac{1}{2}\int_0^{h_2} EI \left[\frac{\partial^2 w}{\partial {x_2}^2}\right]^2 \mathrm{d}\bar{x}_2 = \lfloor W \rfloor^T \frac{1}{2}\int_0^{h_2} E_2 I_2 \lfloor S'' \rfloor^T \lfloor S'' \rfloor \mathrm{d}\bar{x}_2 \lfloor W \rfloor. \qquad (17)$$

Thus, the elemental stiffness matrix is given by

$$K_2{}^j = E_2 I_2 \int_0^{h_2} \lfloor S'' \rfloor^T \lfloor S'' \rfloor \mathrm{d}\bar{x}_2 = \frac{E_2 I_2}{h_2^3} \begin{bmatrix} 0 & 0 & 0 & 0 & 0 & 0 & 0 & 0 \\ 0 & 0 & 0 & 0 & 0 & 0 & 0 & 0 \\ 0 & 0 & 0 & 0 & 0 & 0 & 0 & 0 \\ 0 & 0 & 0 & 0 & 0 & 0 & 0 & 0 \\ 0 & 0 & 0 & 0 & 12 & 6h_2 & -12 & 6h_2 \\ 0 & 0 & 0 & 0 & 6h_2 & 4h_2^2 & -6h_2 & 2h_2^2 \\ 0 & 0 & 0 & 0 & -12 & -6h_2 & 12 & -6h_2 \\ 0 & 0 & 0 & 0 & 6h_2 & 2h_2^2 & -6h_2 & 4h_2^2 \end{bmatrix} \qquad (18)$$

3. Lagrange'S Equation of Motion in Discretized Form

The kinetic energy and the potential energy of the system are obtained by computing the kinetic energy and potential energy of the each element of the system and summing over all the elements. Thus, global mass matrix and global stiffness can be obtained as

$$[M] = \sum_{i=1}^{n_1} \left[M_1^i\right]_g + \sum_{j=1}^{n_2} \left[M_2^j\right]_g \qquad (19)$$

and

$$[K] = \sum_{i=1}^{n_1} \left[K_1^i\right]_g + \sum_{j=1}^{n_2} \left[K_2^j\right]_g \qquad (20)$$

where, $\left[M_1^i\right]_g$, $\left[M_2^j\right]_g$ denote the mass matrices of i^{th} element of first link and j^{th} element of second link respectively expressed in global form and $\left[K_1^i\right]_g$, $\left[K_2^j\right]_g$ denotes the stiffness matrices of i^{th} element of first link and j^{th} element of second link respectively expressed in global form.

Total kinetic energy and potential energy can be expressed as

$$T = \frac{1}{2}[\dot{q}]^T [M][\dot{q}] \text{ and } V = \frac{1}{2}[q]^T [K][q] \qquad (21)$$

respectively, where $[M]$ and $[K]$ are the global matrices and $[q]$ is the global nodal vector defined as $\left[\theta_1 \;\; u_1 \;\; . \;\; . \;\; u_{2n_1+2} \;\; \theta_2 \;\; w_1 \;\; . \;\; . \;\; w_{2n_2+2}\right]$.

Lagrangian of the system is given by $L = T - V$. Then, Lagrange's equations of motion of this dynamic system is written as

$$\frac{\partial}{\partial t}\left[\frac{\partial L}{\partial \dot{\boldsymbol{q}}}\right] - \frac{\partial L}{\partial \boldsymbol{q}} = \boldsymbol{F}_{\boldsymbol{q}}, \qquad (22)$$

where $\boldsymbol{F}_q$ are the generalized forces. Being linear system, global mass and stiffness matrix is constant and equation of motion comes as

$$[M]\{\ddot{q}\} + [K]\{q\} = \{F_q\} \qquad (23)$$

Effect of hub mass and payload mass is incorporated in the global mass matrix and stiffness matrix using Dirac-delta function as described by Dixit *et al.* (2006). Hub mass and tip mass/payload is defined in terms of β (ratio of hub mass to beam mass), μ_2 (ratio of tip mass at link 2 to total beam mass), μ_1 (ratio of tip mass at link 1, mass of the motor at the link joint, to total beam mass) and α (ratio of length of link 2 to length of link 1).

Neglecting load vector, Eq. 23 becomes standard eignvalue problem, which is solved to obtain natural

frequencies of the system. Numerical integration of Eq. 23 is carried out by using Newmark's integration scheme (Dixit, 2009) to obtain transverse deflections u & v, rigid body motions θ_1 & θ_2 and their derivatives.

4. Results and Discussion

In this section, a comparative analysis has been carried out for uniform as well as shape optimized double link flexible revolute manipulator. For the numerical study, a manipulator having uniform diameter 0.01 m, length 1.0 m, mass per unit length 217.3 gm/m, Young's modulus of elasticity 69 GPa is considered for both the links. Damping of the system is neglected. Most of the numerical simulations are done subjected to a sinusoidal torque given in Eq. 24 about the axis of rotation,

$$\left.\begin{aligned} \tau_k &= \tau_{m_k} \sin \pi t, \quad 0 \le t \le 2 \\ &= 0, \qquad\quad 2 < t \le 4 \end{aligned}\right] \; k = 1, 2, \qquad (24)$$

where τ_k, τ_{m_k} and t represent applied torque, torque amplitude and time duration respectively. Torques τ_1 and τ_2 are applied to the hub axis and joint axis respectively.

The dynamic behaviors depend upon many parameters of double links flexible manipulator and also dynamic response consists of several desired objectives *viz* higher hub angle, less static deflection, less residual vibration, less response and settling time, etc. Improved dynamic response is a multi objective problem. Here some parametric study is done to analyze the dynamic behaviour of double link flexible manipulator.

4.1. Dynamic Response due to Different Payloads

Dynamic behaviour of the double link flexible manipulator changes with respect to the change of payloads at the tip of second link as shown in Fig. 4. It is observed that with the increase of payloads, the magnitude of hub angle and joint angle reduce. Residual vibration is considerably more at tip of first link or second link depending upon the input torque at hub joint or link joint respectively.

It is also observed that there is very small effect in dynamic response with the increase of hub inertia. Similar trend is observed in dynamic response due to the variation of motor mass (tip load at link1) and hub mass. For the sake of brevity, these results are not tabulated here.

4.2. Effect of Link Lengths on Dynamic Response

Dynamic response of the double link flexible manipulators also depends upon the links length ratios. For the payloads ratios $\mu_1 = 0.01$, $\mu_2 = 0.02$, $\beta = 5$ and input torques $\tau_{m_1} = 0.2$ N.m and $\tau_{m_2} = 0.04$ N.m, effects of different links length ratios is plotted in Fig. 5, keeping length of the first link constant $(L_1 = 1.0\,\text{m})$. The lesser the length of link 2 with respect to Link 1, the better the dynamic response i.e. more hub/joint angle and lesser residual vibration for the given set of torque. Therefore, designer should not prefer the longer second link with respect to the first link.

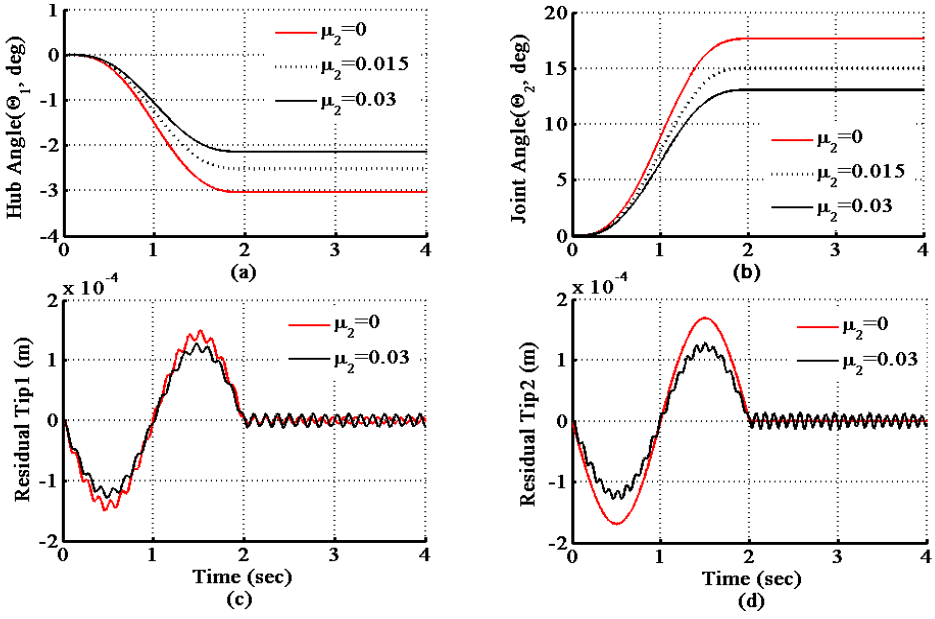

Figure. 4 Dynamic response due to payloads at the tip (a) Hub angle, (b) Joint angle, (c) Residual Tip 1, (d) Residual Tip 2 wit $\mu_1 = 1,\ \beta = 5, \tau_{m_1} = 0$ and $\tau_{m_2} = 0.02$ N.m

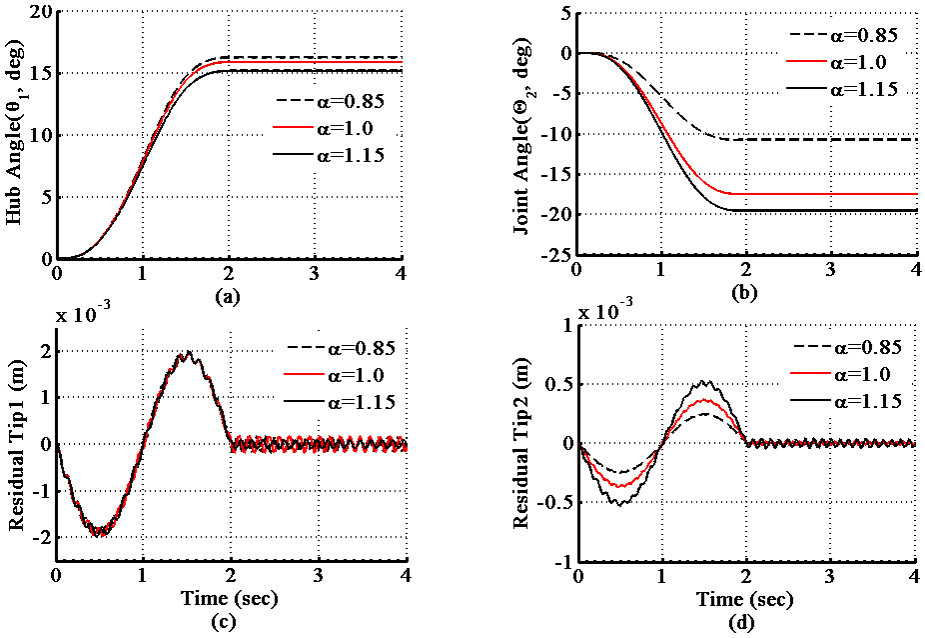

Figure. 5 Dynamic response due to variation of link lengths (a) Hub angle, (b) Joint angle, (c) Residual Tip 1, (d) Residual Tip 2 with $\mu_1 = 0.01, \mu_2 = 0.02, \quad \beta = 5, \tau_{m_1} = 0.2\,\text{N.m}$ and $\tau_{m_2} = 0.04\,\text{N.m}$

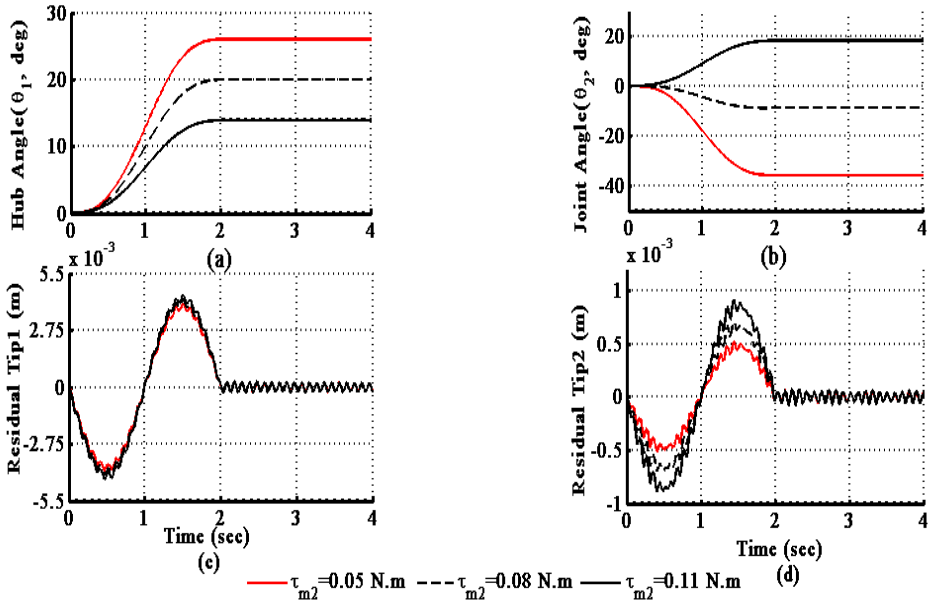

Figure. 6 Dynamic response due to variation of applied torque (a) Hub angle, (b) Joint angle, (c) Residual Tip 1, (d) Residual Tip 2 with $\mu_1 = 0.4, \mu_2 = 0.02, \quad \beta = 5$ and $\tau_{m_1} = 0.4\,\text{N.m}$

4.3. Dynamic Response Due to Different Input Torques

In double link flexible manipulator dynamic response depends upon the magnitude of input torques at the hub and joint between link 1 and two. For the payloads ratios $\mu_1 = 0.4, \quad \mu_2 = 0.02, \quad \beta = 5$ and the input torque $\tau_{m_1} = 0.4\,\text{N.m}$, dynamic response due to the variation of torque τ_2 is plotted in Fig. 6. It is observed that there is a decrease in hub angle and increase of joint angle with the increase of torque amplitude. As the magnitude of applied torque τ_2 increases, there is considerable increment in the residual vibration of the tip of second link. Similar trend is also observed due to the variation of input torque τ_1 at the hub joint (result not shown here). Thus, tip vibration increase for a particular link with the increase of torque amplitude acting in that particular link. Overall angular displacement depends upon the set of input torques at the joints.

4.4. Comparative Dynamic Response due to Different Torque Profile

Different torque profiles shown in Fig. 7 are considered

for the comparison of dynamic response of double link flexible manipulator. All the torque profiles have same amplitude i.e. 0.5 N.m and same duration of excitation i.e. 4 sec. Dynamic response due to different torque profile is shown in Fig. 8.

Triangular torque profile gives the lesser hub angles to the links. Bang-bang torque gives high input energy to the system giving high hub angle as well joint angle. However due to sudden change, bang-bang torque produces high residual vibration to the system. Sinusoidal torque may be preferred for smooth operations of the system.

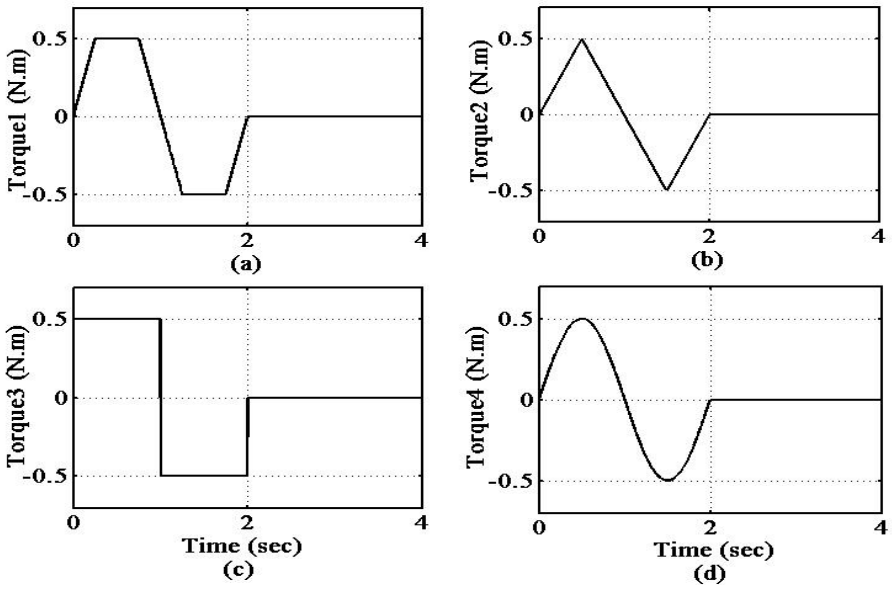

Figure. 7 Different torque profiles (a) Trapezoidal, (b) Triangular, (c) Bang-bang, (d) Sinusoidal

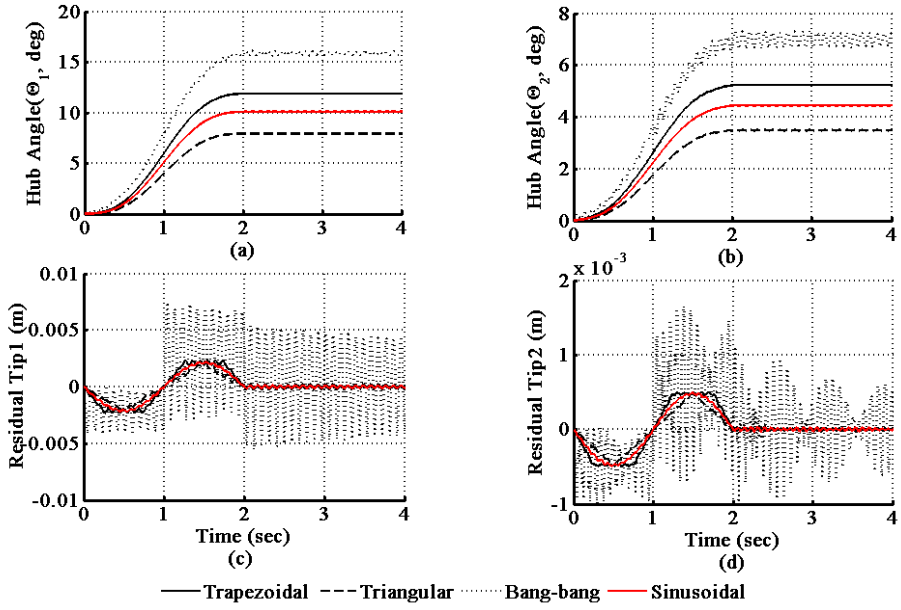

Figure 8 Dynamic response due to different torque profiles (a) Hub angle, (b) Joint angle, (c) Residual Tip 1, (d) Residual Tip 2 with $\mu_1 = 0.02, \mu_2 = 0.02,\ \beta = 5, \tau_{m_1} = 0.2$ N.m and $\tau_{m_2} = 0.06$ N.m .

5. Conclusions

Dynamics of double link flexible manipulator is highly complex and nonlinear in nature. Model is linearized to reduce the complexity of the model and tried to predict the behaviour of the system under low amplitude of vibration due to excitation. Parametric study suggests that dynamic response of the double link manipulator depends upon system parameters viz. payloads at tip and link joint, link lengths, input torque magnitude & profile and hub inertia.

REFERENCES

[1] Ankarah, A., Diken, H. (1997) Vibration control of an elastic manipulator link, J. of Sound and Vib., 204(1), 162-170.

[2] Asada, H, Park, J.H. and Rai. S. (1991) A control-configured flexible arm: Integrated Structure/Control Design, Proceeding of the IEEE International Conference on Robotics and Automation, California , 2356–2362.

[3] Bedoor, B.O.A. and Almusallam, A.A. (2000) Dynamics of flexible links and flexible-joint manipulator, carrying a payload with rotary inertia, Mech. Mach. Theory, 35, 785-820.

[4] Book, W.J., Maizza-Neta O. and Whitney D.E. (1975) Feedback control of two beam, two joint systems with distributed flexibility, ASME J. Dyn. Syst. Meas. Control, 97,424-431.

[5] Chang, L.W. and Hamilton, J.F. (1991) Dynamics of robotic manipulators with flexible links, ASME J. Dyn. Syst. Meas. Control, 113,54-59.

[6] Dixit, U.S. (2009) Finite Element Methods for Engineers, Cengage Learning, Singapore.

[7] Dixit, U.S, Kumar, R., Dwivedy, S.K. (2006) Shape optimization of flexible robotic manipulator, ASME J. of Mechanical Design, 121(3), 559–565.

[8] Dwivedy, S.K. and Eberhard, P. (2006) Dynamic analysis of flexible manipulators: a literature review, J. of Mech. and Mach. Theo., 41, 749-777.

[9] Fu, K.S., Gonzalez, R.C. and Lee, C.S.G. (1987) Robotics: Control, Sensing, Vision, and Intelligence, TMH Edition.

[10] Meghdari, A. and Fahimi, F. (2001) On the first-order decoupling of dynamical equation of motion for elastic multibody systems as applied to a two-link flexible manipulator, Multibody System Dynamics, 5,1-20.

[11] Usoro, P.B., Nadira, R. and Mahil S.S. (1986) A finite element/Lagrange approach to modeling light weight flexible manipulators, ASME J. Dyn. Syst. Meas. Control, 108,198-205.

[12] Wang, F.Y. (1994) On the external fundamental frequencies of one link flexible manipulators, The Intl. J. of Robotics Res., 13,162–170.

[13] Yogit, A.S. (1994) On the stabilty of PD control of a two-link rigid-flexible manipulator, ASME J. Dyn. Syst. Meas. Control,116, 208-215.

[14] Zhang. C. and Bai, G. (2012) Extremum response surface method of reliability analysis on two-link flexible robot manipulator, J. Cent. South Univ., 19, 101-107.